Published in final edited form as:
Small. 2010 December 6; 6(23): 2678–2682. doi:10.1002/smll.201001447.

Gd-Labeled Microparticles in MRI: In Vivo Imaging of Microparticles after Intraperitoneal Injection

Jeremy L. Steinbacher[‡],
Department of Chemistry, University of Vermont, Burlington, VT 05405-0125 (USA)

Sherrill A. Lathrop[‡],
Department of Pathology, University of Vermont, Burlington, VT 05405 (USA)

Kai Cheng,
Department of Chemistry, University of Vermont, Burlington, VT 05405-0125 (USA)

Jedd M. Hillegass,
Department of Pathology, University of Vermont, Burlington, VT 05405 (USA)

Kelly J. Butnor,
Department of Pathology, University of Vermont, Burlington, VT 05405 (USA)

Risto A. Kauppinen,
Biomedical NMR Research Center, Dartmouth-Hitchcock Medical Center, Lebanon, NH 03756 (USA)

Brooke T. Mossman, and
Department of Pathology, University of Vermont, Burlington, VT 05405 (USA)

Christopher C. Landry
Department of Chemistry, University of Vermont, Burlington, VT 05405-0125 (USA)

Christopher C. Landry: Christopher.landry@uvm.edu

Keywords

Mesoporous materials; Silica; Magnetic resonance imaging; Particle excretion; Biomedical applications

Particulate materials have recently been studied for *in vivo* applications such as imaging, drug delivery, and even combined therapy/imaging agents for the simultaneous detection and treatment of diseases.[1–4] Nanoparticles have received much attention in the drug delivery field;[5,6] however, because they can enter organelles and distribute widely throughout the body,[7–10] there is some uncertainty about the acute and/or chronic toxicities of nanoparticles. Microparticles, with their larger size, may be a less toxic alternative that still can be modified with the same array of functionalities as nanoparticles. We recently showed that acid-prepared mesoporous spheres (APMS),[11,12] composed of silica and with an average diameter of 1.5 μm, are readily taken up by cells when modified with tetraethylene glycol (TEG) on their external surfaces. These microparticles also readily deliver chemotherapeutic agents *in vitro* and *in vivo*,[13,14] and can be bifunctionally

Correspondence to: Christopher C. Landry, Christopher.landry@uvm.edu.

‡These authors contributed equally to this work.

Supporting Information is available on the WWW under http://www.small-journal.com or from the author. Materials include complete synthetic and instrumental procedures, additional MR images, and characterization of particles.

modified with both TEG and antibodies for targeted uptake by cancer cells.[15] A unique feature of our microparticles is that they are not present within endosomes after uptake but instead are directly surrounded by cytosol, in contrast to nanoparticles. Thus, molecular cargo including DNA and RNA is released directly to the cytosol and is not subject to the enzymatic and pH-based degradation mechanisms within endosomes. Our current interests include studies on the molecular mechanisms and treatment of malignant mesothelioma (MM)[16] and tumors of the intraperitoneal (IP) cavity, such as pancreatic and ovarian cancers.[17] To visualize our particles *in vivo*, we used a known ligand to immobilize gadolinium(III) to the pores of APMS and imaged animals via magnetic resonance imaging (MRI).[18] *Nanoparticle*-based MRI contrast agents have been reported recently;[19,20] however, we report here for the first time that porous silica *microparticles* containing a Gd chelate can be injected IP and tracked in real-time by MRI. Surprisingly, a fraction of the particles were excreted via the urine, a finding we confirmed by analyzing the urine and tissues of the treated animals.

The initial synthesis of our microparticles was as previously described.[13] Briefly, APMS were synthesized through the acid hydrolysis of tetraethylorthosilicate in an ethanolic aqueous system in the presence of cetyltrimethylammonium bromide as a pore-forming agent. The addition of fluoride nucleated the particles, and after aging 40 min at 100 °C, the particles were filtered and dried; the entire synthesis required less than two hours. TEG was attached to the particle surfaces by modifying the as-synthesized, pore-blocked APMS with a secondary amine alkoxysilane and subsequent reaction with tosyl-TEG. The surfactant was then extracted with ethanol, revealing the pore surfaces. To immobilize the ligand on the pores, a primary amine alkoxysilane was reacted with extracted APMS-TEG and further reaction with diethylenetriamine pentaacetic acid (DTPA) dianhydride yielded the pore-immobilized ligand.[21] Finally, a salt metathesis with $GdCl_3$ in acetate buffer gave Gd-loaded, TEG-modified microparticles as shown schematically and in the scanning electron micrograph in Figure 1. Also shown in Figure 1 are the nitrogen physisorption isotherms and corresponding BET surface areas at subsequent steps in the synthesis of the particles to demonstrate the modification of the pore surfaces with the complex. The loading of Gd was in the range of 4–7 % (w/w), as independently determined by elemental analysis, colorimetric titration of the loading solutions, and thermogravimetric analysis.

We characterized the magnetic properties of the particles by measuring the relaxivities of the particles suspended in agar. The longitudinal relaxivity r_1 at 1.5 T was similar on a per-Gd basis to the soluble DTPA complex of Gd^{3+}, which is the contrast agent in the commercially available Magnevist™ (Table 1). We suspect that the metal complexes in the particles interact with water protons in a manner similar to that of the free complex, but the expected increase in r_1 due to reduced molecular tumbling[22] may be hindered by free rotation of the complex on the surface. Conversely, the enhancement in r_2 is due to the large number of Gd^{3+} ions in the particles, which may behave as a single paramagnetic body. Thus, the paramagnetic particles create local magnetic inhomogeneities in the surrounding environment, readily dephasing surrounding water protons and increasing r_2 relaxivity. To confirm that the immobilized Gd complex was stable in an aqueous environment, we performed leaching experiments by soaking particles loaded with the Gd complex in pH 7.4 PBS buffer and periodically measuring the amount of released Gd^{3+} by colorimetric titration. For comparison, we prepared Gd-MCM-41 prepared by the addition of Gd directly to the synthesis mixture (unchelated), as described in the literature.[23,24] Consistent with previous reports,[20] our particles released no measurable Gd^{3+} for up to 40 days, while the Gd-MCM-41 leached most of the adsorbed Gd^{3+} over the same time span.

After characterizing the physical and magnetic properties of the Gd-loaded TEG-modified microparticles and satisfied with the stability of the Gd complex, we moved to IP injection

of the particles into Wistar rats. Imaging was performed on a 7 T MRI scanner at Dartmouth Medical School designed for rodents. Based on the relaxivity per Gd^{3+} ion shown above, we used a particle dose of 500 mg kg^{-1} (= 213 μmol Gd kg^{-1}), similar to the Gd dose typically administered using Magnevist™.[20] Baseline images were acquired, injections were made via cannulae into the lower-left quadrant of the IP cavity and images were acquired immediately post-injection and at 2, 4, 25, and 144 hours (Figure 2). Significant contrast was observed in the bladder within 2 h, a signal that persisted to 25 h. The signal enhancement implied that the microparticles were within the bladder, which was unanticipated because the kidneys were expected to filter out proteins and particles larger than roughly 3–10 nm in diameter.[25–28] Other groups have delivered microparticles, typically biodegradable polyesters, to the IP cavity, but excretory pathways were not elucidated because the particles were meant to remain in the body and degrade over the span of weeks.[29,30] To the best of our knowledge, only one other report examined the IP injection of porous silica microparticles, and the fate of those particles was elucidated post-mortem.[31] Thus, these data represent the first real-time imaging of the biodistribution of silica microparticles after IP injection.

Additional MR images and post-mortem examinations of kidney and bladder tissues helped to show that the enhanced contrast seen in the bladders was truly caused by Gd-loaded silica, as opposed to free Gd^{+3} that could have leached from the particles.[32] Although sagittal images could not be acquired on the 7 T instrument, views of a C57BL/6 mouse acquired on a clinical 3 T MRI scanner at the University of Vermont roughly 30 minutes post-injection showed a bowl-shaped region of contrast on the posterior hemisphere of the bladder, indicating that the particles were settling as the mouse lay immobilized on its back (Figure 3). Interestingly, the ureter was clearly illuminated by the contrast agent. A three-dimensional reconstruction of a stack of coronal images of a mouse 4 hr post-injection with 500 mg kg^{-1} of Gd-loaded APMS also revealed a bowl-shaped appearance of the bladder (see Supporting Information), again suggesting that the particles had settled on the bottom of the bladder under the influence of gravity. Post-mortem examination of kidney and bladder tissue confirmed the presence of the particles in these organs. An SEM image of a renal tubule showed micron-sized spheres *on the inside* of the tubule; likewise, examination of the bladder showed particles on the interior surface.[33] Taken together, these results are consistent with the idea that the Gd-loaded microparticles passed through the kidney into the bladder.

Direct evidence that the microparticles themselves—and not simply unchelated Gd^{3+}—were excreted through the bladder came from analyzing the urine of the rats after each imaging time point. The urine was processed by a bleach treatment to digest proteinaceous material and microfiltration to collect any remaining solids. SEM images of the processed urine showed particle-shaped objects that were confirmed to be Gd-loaded APMS using energy dispersive X-ray spectroscopy (EDS) to detect silicon and gadolinium (Figure 4). EDS indicated strong signals from Si and Gd when targeted on-particle, but greatly attenuated signals when targeted off-particle.[34] Finally, we note that none of the 8 animals injected with Gd-loaded APMS in the IP cavity exhibited signs of Gd^{3+} toxicity for one week post-injection.[35,36] Thus, the particles did enter the bladder and were subsequently excreted after IP injection, with clearance to below the detection limit of the MRI scanner by six days post-injection. At this point, it is not known with certainty how the microparticles entered the bladder, but our data strongly suggest particle excretion by the kidney, given that the bladder and ureters are lined with impenetrable smooth muscle tissue.[37,38] It is possible that the particles could be filtered across the glomerulus or be secreted across the renal tubules. Indeed, renal epithelial cells along the nephron are capable of transcytosis,[39–41] and our *in vitro* experience with APMS shows it is rapidly endocytosed by a variety of cell types.[13] If APMS could gain access to the peritubular interstitium of the kidney, entrance

into the renal tubule (e.g., via endocytosis, or less likely, secretion) with subsequent flow into the collecting ducts and ultimately into the bladder could occur. We currently favor this model because enhanced contrast was not observed in the vasculature after IP injection of the particles,[33] rendering a direct blood-borne route into the kidneys via glomerular ultrafiltration unlikely.

Regarding the toxicity of our particles, preliminary dose-escalation studies using 1.0 to 700 mg kg^{-1} of Gd-loaded microparticles in mice resulted in no negative consequences on behavior (feeding, grooming, etc.). For example, a Wistar rat exhibited healthy exploration behavior approximately an hour after an IP injection of 500 mg kg^{-1} (see video in Supporting Information). Moreover, post-mortem examinations one week after the injection of particles revealed no gross pathological abnormalities as determined by a board-certified pathologist, who found no necrosis in all organs treated with standard histological staining (details are in the Experimental Section). In the broader scope of particle-based therapies, our particles appear to be less toxic after IP injection than common types of amorphous silica nanoparticles (MCM-41, SBA-15, and a non-spherical micron-sized silica)[31] despite being composed of the same material.[42] Thus, we suggest that the larger diameter, spherical morphology, and surface modification of APMS-TEG prevents interactions with cellular organelles,[13] unlike some nanoparticle formulations that can disrupt normal cellular functions.[43–46] Also, the larger size of microparticles helps to mitigate cellular sensitivity to the exact size and chemical modification of nanoparticles and the biological setting of their interactions.[45,46]

These results show that porous silica microparticles could be used as transient, excretable IP drug-delivery devices, contrary to the popular sentiment that particle-based biomaterials should be in the nano-scale to facilitate circulation and excretion from the body.[25,47] While microparticulate drug-delivery vehicles may not be suitable for every application, our findings have important implications for other microparticle-based drug delivery vehicles and for injectable particle systems in general. We are currently working to elucidate the details of the mechanism of excretion and to determine what fraction of the total dose was passed via the urine. Moreover, we are using drug-loaded APMS particles in a murine tumor xenograft model of mesothelioma and implementing targeted drug delivery *in vivo* with antibody-labeled particles.

Experimental Section

Characterization of Particles

Thermogravimetric analysis (TGA) was performed on a Perkin-Elmer Pyris 1 TGA. Scans were performed under a continuous flow of air (40 mL min^{-1}) with the following method: 25–100 °C at 40 °C min^{-1}, isothermal at 100 °C for 10 minutes, and 100–800 °C at 10 °C min^{-1}. N_2 adsorption and desorption isotherms were obtained on a Micromeritics TriStar instrument. Surface areas were measured using the BET method and pore size distributions were calculated from a modified KJS method using the adsorption branch.[48–50] SEM samples were dusted onto carbon tape applied to aluminum sample stubs that were then sputter coated with Pd/Au for 3.5 minutes. SEM images were obtained using a JEOL 6060 scanning electron microscope operating at an accelerating voltage of 25 kV or a JEOL 1210 scanning transmission electron microscope operating at an accelerating voltage of 20 kV to acquire EDS spectra.

Relaxivity Measurements

Relaxation times were measured at 60 MHz and 37 °C on a Bruker mq60 NMR Analyzer (Billerica, MA). A stock solution in water was prepared from dry APMS-DTPA/Gd-TEG particles and further diluted to make five aqueous suspensions of concentrations 0.125 – 2

mM Gd. Water was purified using a Millipore Milli-Q Synthesis water system (Billerica, MA). Each suspension was embedded in 1% agarose gel to avoid settling of particles and resulted in final Gd concentrations of approximately 0.0625 – 1 mM Gd. An inversion-recovery pulse sequence was used to measure the longitudinal (T_1) relaxation times, while a cpmg or spin echo pulse sequence was used to measure transverse (T_2) relaxation times. Relaxation times were determined using monoexponential curve fitting of 10 data points (4 averages for each point). The relaxivity was determined by taking the slope of a plot of $1/T_n$ (n = 1, 2) versus concentration. Control APMS-TEG particles and Gd^{3+}-DTPA were measured in the same manner. Gadolinium concentrations were verified using inductively-coupled plasma mass spectrometry on a Thermo Electron Corporation $XSeries^{II}$ ICP-MS with Thermo PlasmaLab software (Waltham, MA).

MR Imaging

MRI experiments were preformed in a horizontal bore scanner (90 mm) with 55 gauss cm^{-1} gradient strength, (Magnex Scientific Ltd., Abingdon, UK) at 7 Tesla interfaced to a Varian Unity INOVA console (Varian Inc., Palo Alto, CA, USA) and a transmit/receive volume coil operating in quadrature with an active depth of approximately 6 cm. (TR = 1.2 s, effective TE = 10 ms, matrix size 128×128 voxels, field of view = 8×6 cm, 20 slices, no gap, with slice thickness of 1 mm, signal averaging 4 scans and 4 steady state scans). Images were acquired with a conventional spin echo T1-weighted, fat-suppressed pulse sequence.

Animal Injections

All animal studies were approved by the Institutional Animal Care and Use Committees at the University of Vermont and Dartmouth Medical School. After anesthesia using 3% isoflourane, Wistar rats (N=2) or C57BL/6 mice (N=6) were cannulated through the lower left wall of the IP cavity. Cannula tubing was secured in place with tape, and the animal was then placed in a holding tray to minimize movement. Due to differences in the trays used to secure the animals, mice were positioned ventral side up while rats were positioned dorsal side up. The animal-bearing tray was then placed in the bore of the MRI scanner and shimming was preformed followed by pre-particle administration image acquisition. The APMS-DTPA/Gd-TEG particles, suspended in saline (0.9 %) at a dose of 500 mg kg^{-1} (typically 100 mg for a 0.2 kg rat), were then injected through the cannula tubing into the peritoneal cavity followed by a flush of 100–200 μl of saline to ensure no particles remained within the tubing. Images were acquired for the 0 hr time point, i.e. immediately following injection. Following image acquisition the animal was removed from the MRI and placed on a heated water pad; any urine expelled was collected with a fresh, sterile syringe and was placed in sterile Eppendorf tubes. Urine was stored at 4 °C until digestion and filtration were completed. The animal was allowed to recover from the anesthesia and provided food and water *ad libitum* before collection of additional images at 2, 4, 25, and 144 hr. All animals were euthanized after the final imaging session at 1 week. Mice were euthanized by a 0.1ml injection of sodium pentobarbital and rats were euthanized by cervical dislocation. Urine, if remaining in the bladder, was collected for further analysis using 1.0 mL sterile syringes. Necropsies were performed on each animal and did not reveal any abnormalities in organ appearance. Histology (H&E) of paraffin-embedded sections of each organ including heart, liver, lung, spleen, kidney, and bladder was examined by a board-certified pathologist (Kelly J. Butnor, M.D.). The portal duct of the liver from the rats showed a mild infiltrate of eosinophils. Sections of the spleen revealed a mild increase of eosinophils in the sinusoids, and examination of lung sections showed a mild peribronchial infiltrate of eosinophils. None of the organs examined showed necrosis or apparent damage due to the administration of APMS-DTPA/Gd-TEG.

Urinalysis

Urine samples were added to 15 ml conical tubes and digested in bleach (4 ml), rocking at room temperature for 2 hr. Digested samples were then filtered through a 0.4 μm cellulose filter (Whatman) followed by 5 rinses with H_2O and 100% ethanol. Filters were dried at room temperature overnight in a desiccator. A representative section of the dried filter was removed with a razor blade, and the sections were mounted onto copper planchets using parlodion (2%) in amyl acetate and were then sputter coated with gold and palladium (3–4 min) in a Polaron sputter coater (Model 5100; Quorum Technologies, Guelph, ON, Canada).

APMS functionalized on its external surface with TEG (APMS-TEG)

This material was synthesized as described elsewhere[13] and in the supporting information.

APMS internally functionalized with amine and externally functionalized with TEG (APMS-NH_2-TEG)

APMS-TEG (1.0 g) were added to 50 mL hexanes along with 200 μL (3-aminopropyl)triethoxysilane (APTES) and the suspension was refluxed for twenty-four hours under a nitrogen atmosphere. The particles were filtered, washed repeatedly with hexanes, and dried under vacuum.

APMS internally functionalized with chelating ligand and externally functionalized with TEG (APMS-DTPA-TEG)

APMS-NH_2-TEG (1.0 g) were added to 10 mL dry *N*,*N*-dimethylformamide in a round-bottom flask equipped with a condenser and a side-arm stopcock. Separately, diethylenetriamine pentaacetic acid dianhydride (DTPA, 180 mg, 0.5 mmol) was dissolved in 5 mL dimethyl sulfoxide. Finally, the DTPA/DMSO solution and triethylamine (140 μL, 1.0 mmol) were added to the particle suspension via syringes. The suspension was then stirred at 40 °C under a nitrogen atmosphere for 24 hours. At this time, 2 mL of water was added and stirring was continued for another two hours. The particles were isolated by filtration and washing with methanol (4 × 5 mL) before drying under vacuum.

APMS internally functionalized with chelated Gd^{+3} and externally modified with TEG (APMS-DTPA/Gd-TEG)

APMS-DTPA-TEG (0.5 g) were suspended in 10 mL of a sodium acetate buffer (10 mM, pH = 6.5) and briefly sonicated. A solution of $GdCl_3$•$6H_2O$ in deionized water (50 mM) was added such that roughly 1.1 equivalents of Gd was added relative to immobilized DTPA ligands as calculated from TGA curves of the APMS-DTPA-TEG. The suspension was stirred at room temperature for four hours, and the particles were isolated by filtration and repeated washing with the same acetate buffer (4 × 5 mL) and deionized water (3 × 5 mL) before vacuum drying.

Supplementary Material

Refer to Web version on PubMed Central for supplementary material.

Acknowledgments

This project was funded by the National Institutes of Health under grant numbers T32ES0071 and 1R41-CA126155-01A1 and by the Mesothelioma Applied Research Foundation. We thank M. von Turkovich and the UVM Microscopy Imaging Center, T. J. Meade and E. A. Schultz-Sikma for relaxivity measurements, and M. Lathrop, N. Jerome, K. Hekmatyar, and S. Beuschel for assistance with the experiments.

References

1. Niemeyer CM. Angew. Chem.-Int. Edit. 2001; 40:4128.
2. Kim J, Piao Y, Hyeon T. Chem. Soc. Rev. 2009; 38:372. [PubMed: 19169455]
3. Vallet-Regi M, Balas F, Arcos D. Angew. Chem.-Int. Edit. 2007; 46:7548.
4. Slowing, Vivero-Escoto JL, Wu CW, Lin VSY. Adv. Drug Deliv. Rev. 2008; 60:1278. [PubMed: 18514969]
5. De M, Ghosh PS, Rotello VM. Adv. Mater. 2008; 20:4225.
6. Rosi NL, Mirkin CA. Chem. Rev. 2005; 105:1547. [PubMed: 15826019]
7. Lewinski N, Colvin V, Drezek R. Small. 2008; 4:26. [PubMed: 18165959]
8. Fitzpatrick JAJ, Andreko SK, Ernst LA, Waggoner AS, Ballou B, Bruchez MP. Nano Lett. 2009
9. Oberdorster G, Stone V, Donaldson K. Nanotoxicology. 2007; 1:2.
10. Handy RD, Owen R, Valsami-Jones E. Ecotoxicology. 2008; 17:315. [PubMed: 18408994]
11. Gallis KW, Araujo JT, Duff KJ, Moore JG, Landry CC. Adv. Mater. 1999; 11:1452.
12. Gallis, KW.; Landry, CC. United States Patent. 6,334,988. 2002.
13. Blumen SR, Cheng K, Ramos-Nino ME, Taatjes DJ, Weiss DJ, Landry CC, Mossman BT. Am. J. Respir. Cell Mol. Biol. 2007; 36:333. [PubMed: 17038662]
14. Hillegass JM, Blumen SR, Cheng K, MacPherson MB, Aleexeva V, Lathrop SA, Beuschel SL, Steinbacher JL, Butnor KJ, Ramos-Nino ME, Shukla A, James TA, Weiss DJ, Taatjes DJ, Landry CC, Mossman BT. Int. J. Cancer. 2010 accepted.
15. Cheng K, Blumen SR, MacPherson MB, Steinbacher JL, Mossman BT, Landry CC. ACS Appl. Mater. Interface. 2010
16. Hesdorffer ME, Chabot JA, Keohan ML, Fountain K, Talbot S, Gabay M, Valentin C, Lee SM, Taub RN. Am. J. Clin. Oncol.-Cancer Clin. Trials. 2008; 31:49.
17. Hassan R, Ho M. Eur. J. Cancer. 2008; 44:46. [PubMed: 17945478]
18. Caravan P, Ellison JJ, McMurry TJ, Lauffer RB. Chem. Rev. 1999; 99:2293. [PubMed: 11749483]
19. Na HB, Song IC, Hyeon T. Adv. Mater. 2009; 21:2133.
20. Taylor KML, Kim JS, Rieter WJ, An H, Lin WL, Lin WB. J. Am. Chem. Soc. 2008; 130:2154. [PubMed: 18217764]
21. Ladd DL, Hollister R, Peng X, Wei D, Wu G, Delecki D, Snow RA, Toner JL, Kellar K, Eck J, Desai VC, Raymond G, Kinter LB, Desser TS, Rubin DL. Bioconjugate Chem. 1999; 10:361.
22. Caravan P. Chem. Soc. Rev. 2006; 35:512. [PubMed: 16729145]
23. Grun M, Unger KK, Matsumoto A, Tsutsumi K. Microporous Mesoporous Mat. 1999; 27:207.
24. Lin YS, Hung Y, Su JK, Lee R, Chang C, Lin ML, Mou CY. J. Phys. Chem. B. 2004; 108:15608.
25. Stolnik S, Illum L, Davis SS. Adv. Drug Deliv. Rev. 1995; 16:195.
26. Drumond MC, Deen WM. Am. J. Physiol. 1994; 266 F1.
27. Lea PJ, Silverman M, Hegele R, Hollenberg MJ. Microvasc. Res. 1989; 38:296. [PubMed: 2607999]
28. Kondo H. J. Electron. Micr. Tech. 1990; 14:63.
29. O'Hagan DT, Rahman D, McGee JP, Jeffery H, Davies MC, Williams P, Davis SS, Challacombe SJ. Immunology. 1991; 73:239. [PubMed: 2071168]
30. Jones DH, Corris S, McDonald S, Clegg JCS, Farrar GH. Vaccine. 1997; 15:814. [PubMed: 9234522]
31. Hudson SP, Padera RF, Langer R, Kohane DS. Biomaterials. 2008; 29:4045. [PubMed: 18675454]
32. Sarka L, Burai L, Brucher E. Chem.-Eur. J. 2000; 6:719.
33. Lathrop SA, Steinbacher JL, Cheng K, Hillegass JM, Bueschel S, MacPherson MB, Butnor K, Kauppinen RA, Landry CC, Mossman BT. 2010 in preparation.
34. The residual silicon signal resulted from partial dissolution of the particles during the bleach digestion. Alternative digestion procedures that avoided bleach did not result in the silicon residue on the filter but yielded messy, salt-contaminated SEM samples (Supporting Information, Figure S14).

35. Haley TJ, Raymond K, Komesu N, Upham HC. Brit. J. Pharmacol. 1961; 17:526.
36. Adding LC, Bannenberg GL, Gustafsson LE. Cardiovasc. Drug Rev. 2001; 19:41. [PubMed: 11314600]
37. Andersson KE, Arner A. Physiol. Rev. 2004; 84:935. [PubMed: 15269341]
38. Weiss RM. Am. J. Kidney Dis. 1983; 2:409. [PubMed: 6337478]
39. Bens M, Vandewalle A. Pflugers Arch. 2008; 457:1. [PubMed: 18427833]
40. Reilly RF, Ellison DH. Physiol. Rev. 2000; 80:277. [PubMed: 10617770]
41. Thomas SR, Layton AT, Layton HE, Moore LC. Proc. IEEE. 2006; 94:740.
42. Mossman BT, Churg A. Am. J. Respir. Crit. Care Med. 1998; 157:1666. [PubMed: 9603153]
43. Buzea C, Pacheco, Robbie K. Biointerphases. 2007; 2 MR17.
44. Casals E, Vazquez-Campos S, Bastus NG, Puntes V. Trac-Trends Anal. Chem. 2008; 27:672.
45. Nel A, Xia T, Madler L, Li N. Science. 2006; 311:622. [PubMed: 16456071]
46. Oberdorster G, Oberdorster E, Oberdorster J. Environ. Health Perspect. 2005; 113:823. [PubMed: 16002369]
47. Awasthi VD, Garcia D, Goins BA, Phillips WT. Int. J. Pharm. 2003; 253:121. [PubMed: 12593943]
48. Kruk M, Antochshuk V, Jaroniec M, Sayari A. J. Phys. Chem. B. 1999; 103:10670.
49. Kruk M, Jaroniec M, Sakamoto Y, Terasaki O, Ryoo R, Ko CH. J. Phys. Chem. B. 2000; 104:292.
50. Kruk M, Jaroniec M, Sayari A. Langmuir. 1997; 13:6267.

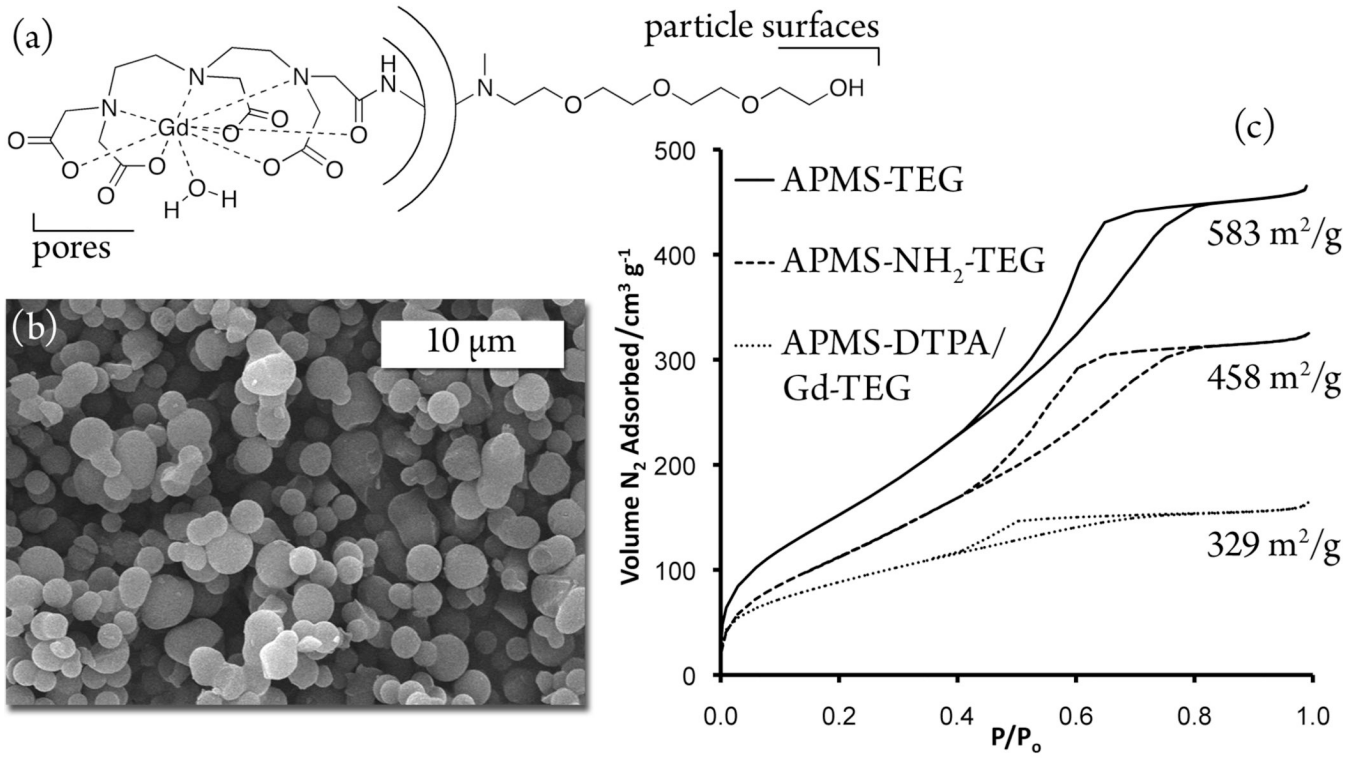

Figure 1.
(a) Illustration of the modified microparticles, (b) SEM image of Gd-loaded microparticles, and (c) N_2 physisorption isotherms and BET surface areas at subsequent stages of the synthesis.

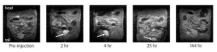

Figure 2.
Magnetic resonance images of one Wistar rat injected IP with Gd-loaded microparticles, focusing on the lower abdominal cavity. Enhanced contrast in the bladder at early time points is indicated by the arrows, showing that a fraction of the microparticles were excreted in the urine.

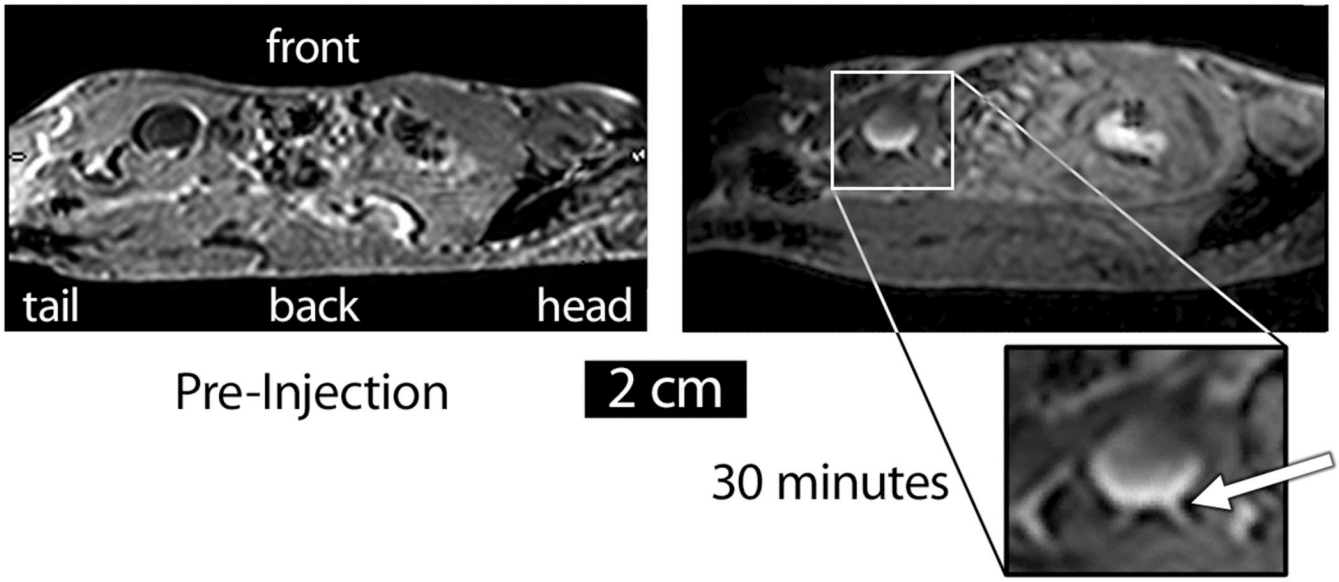

Figure 3.
Sagittal MR image of a C57BL/6 mouse injected IP with APMS-DTPA/Gd-TEG. The particles appear as a bowl-shaped region of contrast in the bladder, and the ureter is also visible (white arrow). Because the animal was lying on its back, these images suggest that the particles were settling under the influence of gravity.

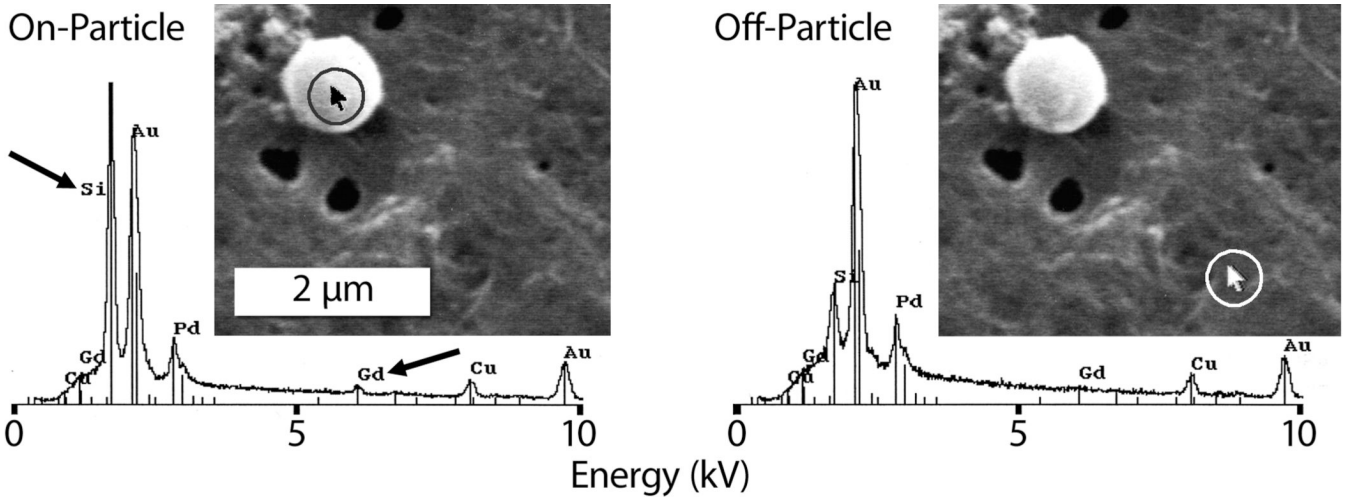

Figure 4.
SEM and EDS analyses (probe target highlighted in circles) of rat urine excreted at 2 hr, showing Gd-loaded APMS microparticles.

Table 1

Relaxivities (mM^{-1} s^{-1}) of APMS-DTPA/Gd-TEG and soluble DTPA/Gd suspended in agar at a field strength of 1.5 T.

Sample	r_1 (per Gd)	r_2 (per Gd)
APMS/Gd	2.8 ± .2	23 ± 2
$DTPA/Gd_{(aq)}$	2.9 ± .2	2.9 ± .2